Estimation of RIS Misorientation in both Near and Far Field Regimes

Don-Roberts Emenonye, Harpreet S. Dhillon, and R. Michael Buehrer

***Abstract*—This paper presents a rigorous examination of the estimation of the misorientation of a reconfigurable intelligent surface (RIS) based on the received signal when the user equipment (UE) is in the near or far fields of the RIS. The Bayesian analysis views the location of the RISs as *a priori* system-level information. With incorrect *a priori* information, the position and orientation offsets of the RISs become parameters that need to be estimated and fed back to the Base station (BS) for correction. Two key insights are obtained from our Bayesian analysis. First, the Bayesian equivalent Fisher information matrix (EFIM) for the channel parameters indicates that the RIS orientation offset cannot be estimated when there is an unknown phase offset in the received signal in the far-field propagation regime. Second, the corresponding EFIM for the channel parameters in the received signal observed in the near-field shows that this unknown phase offset does not hinder the estimation of the RIS orientation offset when the UE has more than one receive antenna.**

I. Introduction

A reconfigurable intelligent surface (RIS) is a planar surface comprising of sub-wavelength-sized meta-materials capable of controlling a wireless propagation channel by applying a desired transformation on the incoming signal through the software control of each meta-material. This unique ability to control harsh wireless channels has led to many works investigating the information available in the signals received after reflections from one or more RISs [1]–[11]. These prior works on the quantification of the information in RIS-aided systems can be grouped mainly into i) continuous RIS [3]–[5] and discrete RIS [6]–[10], and ii) near-field [3]–[8] and far-field propagation [9]–[11]. Although the general quantification of the information available in the signals received after reflections from RISs has been well established in the recent literature, the fundamental difference in the quantification of this available information in the near and far field propagation regimes under the effect of RIS misorientation has not been investigated, which is the main topic of this paper.

In this paper, we incorporate uncertainties in RIS location by strictly viewing the position and orientation of one or more RISs as *a priori* system-level information and subsequently present a derivation of the general FIM for the channel parameters present in the received signals. This viewpoint presents the opportunity of investigating the estimation of RIS orientation offset at the receiver. We analyze the possibility of estimating this offset through the developed Bayesian framework under both near-field and far-field propagation regimes. First, we rigorously show that with no *a priori* information about the channel parameters, when the signal reflected from a misoriented RIS is received in the far-field with an unknown phase offset, the resulting general FIM containing both the orientation offset and the unknown phase offset is rank deficient. This result indicates that irrespective of the number of receive antennas at the user equipment (UE), in the absence of *a priori* information about the unknown phase offset, the orientation offset of an RIS can not be estimated and corrected in the far-field. Second, we show that the rank deficiency observed in the FIM containing both the orientation offset and the unknown phase offset for the far-field is not observed in the corresponding FIM for the near-field with more than one receive antenna. This result is non-trivial as *a priori* information about an unknown phase offset is challenging to obtain. Hence, practically, the possibility of estimating and correcting the RIS orientation offset through the received signal at the UE only exists in the case of near-field propagation.

D.-R. Emenonye, H. S. Dhillon and R. M. Buehrer are with Wireless@VT, Bradley Department of Electrical and Computer Engineering, Virginia Tech, Blacksburg, VA, 24061, USA. Email: {donroberts, hdhillon, rbuehrer}@vt.edu. The support of the US National Science Foundation (Grants ECCS-2030215 and CNS-2107276) is gratefully acknowledged. The extended journal version of this paper is available at [1].

II. Misorientation Aware System Model

We consider the downlink of an RIS-assisted single-input multi-output (SIMO) system operating with a single antenna base station (BS), $N_R^{[m]}$ reflecting elements at the m^{th} RIS where $m \in \mathcal{M}_1 = \{1, 2, \cdots, M_1\}$, and N_U antennas at the UE. This paper occasionally refers to the BS, RISs, and UE as communication entities. The V^{th} entity has an arbitrary but known array geometry and the centroid of this entity is *initially* located at $\tilde{\boldsymbol{p}}_V = [\tilde{x}_V, \tilde{y}_V, \tilde{z}_V]^{\mathrm{T}} \in \mathbb{R}^3$, the v^{th} element on this entity is initially located at $\tilde{\boldsymbol{s}}_v \in \mathbb{R}^3$. The point, $\tilde{\boldsymbol{s}}_v$, is defined with respect to the centroid of the V^{th} entity and is uniquely represented with respect to the global origin as $\tilde{\boldsymbol{p}}_v = \tilde{\boldsymbol{p}}_V + \tilde{\boldsymbol{s}}_v$. A representation in matrix form of the points describing all the elements on the V^{th} entity is $\tilde{\boldsymbol{S}}_v = [\tilde{\boldsymbol{s}}_1, \tilde{\boldsymbol{s}}_2, \cdots, \tilde{\boldsymbol{s}}_{N_V}]$, where N_V is the number of elements on the V^{th} entity. For the RISs, the initial location refers to the location at deployment and can be assumed to be known. On the other hand, the knowledge of the initial location of the UE is application dependent. These initial locations might change with time even though the network might still think that these entities are at their initial locations, thereby resulting in what we call *misorientation*. The effect is particularly prominent when some of these entities, such as RISs, are deployed indoors or on movable objects [10], [12]. It is important to note that the BS is completely fixed

and can not be misoriented. Note that the above setup lends generality to our analysis by making it agnostic to the exact reason behind misorientation. The new (misoriented) position of an element on a given entity is

$$\begin{aligned} \boldsymbol{p}_v &= \tilde{\boldsymbol{p}}_V + \boldsymbol{Q}_V \tilde{\boldsymbol{s}}_v, \\ \boldsymbol{p}_v &= \boldsymbol{p}_V + \boldsymbol{s}_v, \end{aligned} \tag{1}$$

where $\boldsymbol{p}_V = [x_V, y_V, z_V]^{\mathrm{T}} = \tilde{\boldsymbol{p}}_V$, $\boldsymbol{s}_v = \boldsymbol{Q}_V \tilde{\boldsymbol{s}}_v$, $\boldsymbol{Q}_V = \boldsymbol{Q}(\alpha_V, \psi_V, \varphi_V)$ defines a 3D rotation matrix [13]. The orientation angles of the V^{th} entity are vectorized as $\boldsymbol{\Phi}_V = [\alpha_V, \psi_V, \varphi_V]^{\mathrm{T}}$. In matrix form, all the points describing the elements on the V^{th} entity that has been misoriented are collectively represented as $\boldsymbol{S}_v = [\boldsymbol{s}_1, \boldsymbol{s}_2, \cdots, \boldsymbol{s}_{N_V}]$.

The position of the V^{th} entity's centroid located at $\boldsymbol{w}_V$ can be described in relation to the position of the G^{th} entity's centroid located at $\boldsymbol{w}_G$ as $\boldsymbol{w}_V = \boldsymbol{w}_G + d_{\boldsymbol{w}_G \boldsymbol{w}_V} \boldsymbol{\Delta}_{\boldsymbol{w}_G \boldsymbol{w}_V}$, where $\boldsymbol{w} \in \{\boldsymbol{p}, \tilde{\boldsymbol{p}}\}$, $d_{\boldsymbol{w}_G \boldsymbol{w}_V}$ is the distance from point $\boldsymbol{w}_G$ to point $\boldsymbol{w}_V$ and $\boldsymbol{\Delta}_{\boldsymbol{w}_G \boldsymbol{w}_V}$ is the corresponding unit direction vector $\boldsymbol{\Delta}_{\boldsymbol{w}_G \boldsymbol{w}_V} = [\cos\phi_{\boldsymbol{w}_G \boldsymbol{w}_V} \sin\theta_{\boldsymbol{w}_G \boldsymbol{w}_V}, \sin\phi_{\boldsymbol{w}_G \boldsymbol{w}_V} \sin\theta_{\boldsymbol{w}_G \boldsymbol{w}_V}, \cos\theta_{\boldsymbol{w}_G \boldsymbol{w}_V}]^{\mathrm{T}}$. The points corresponding to the v^{th} element on the V^{th} entity is defined as $\boldsymbol{w}_v = d_{\boldsymbol{w}_v} \boldsymbol{\Delta}_{\boldsymbol{w}_v}$, where $\boldsymbol{w} \in \{\boldsymbol{s}, \tilde{\boldsymbol{s}}\}$, $d_{\boldsymbol{w}_v}$ is the distance from the centroid of the V^{th} entity to its v^{th} element, and $\boldsymbol{\Delta}_{\boldsymbol{w}_v}$ is the corresponding unit direction vector, $\boldsymbol{\Delta}_{\boldsymbol{w}_v} = [\cos\phi_{\boldsymbol{w}_v} \sin\theta_{\boldsymbol{w}_v}, \sin\phi_{\boldsymbol{w}_v} \sin\theta_{\boldsymbol{w}_v}, \cos\theta_{\boldsymbol{w}_v}]^{\mathrm{T}}$.

In the rest of this paper, we assume that there are at least $M \geq 2$ paths between the BS and the u^{th} UE antenna. The LOS path is blocked, and the remaining paths are the RIS paths provided to the u^{th} UE antenna through the RISs (see Fig. 1). All other paths from natural scatters or natural reflectors are assumed to be much weaker than the RIS paths. Hence, these paths are ignored in this paper.

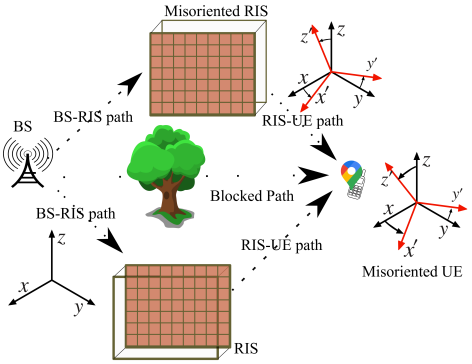

Fig. 1. An illustration of the system model.

A. General Signal Representation

We consider the transmission of T Orthogonal frequency division multiplexing (OFDM) symbols, each containing N subcarriers. The BS transforms the signal to the time domain using an $N-$point inverse fast Fourier transforms (IFFT), and adds a cyclic prefix of sufficient length N_{cp} to the transformed symbols. In the time domain, this cyclic prefix has length $T_{cp} = N_{cp} T_s$ where $T_s = 1/B$ represents the sampling period, and the final transmitted symbol during the n^{th} subcarrier is $x[n]$. At the receiver, after the removal of the cyclic prefix and the application of an N-point fast Fourier transform (FFT) to the t^{th} received OFDM symbol, the signal at the n^{th} subcarrier can be described as

$$\begin{aligned} y_{t,u}[n] &= \mu_{t,u}[n] + n_{t,u}[n], \\ &\sum_{m=1}^{M_1} \gamma_t^{[m]} \beta^{[m]} \rho^{[m]} \sum_{r=1}^{N_R^{[m]}} e^{j\vartheta_r^{[m]}} e^{-j2\pi f_n (\tau_{\boldsymbol{b}_B \boldsymbol{r}_r}^{[m]} + \tau_{\boldsymbol{r}_r \boldsymbol{u}_u}^{[m]})} x[n] \\ &+ n_{t,u}[n], \end{aligned} \tag{2}$$

where $\{\boldsymbol{b}, \boldsymbol{r}, \boldsymbol{u}\} \in \{\boldsymbol{p}, \tilde{\boldsymbol{p}}\}$, $\mu_{t,u}[n]$ and $n_{t,u}[n] \sim \mathcal{CN}(0, N_0)$ are the noise-free part (useful part) of the signal and the Fourier transformed thermal noise local to the UE's antenna array, respectively. Here, $\mathbf{p}$ is used for entities that are misoriented and $\tilde{\mathbf{p}}$ is used for the entities that are at their original locations. The pathloss of the m^{th} RIS path is $\rho^{[m]} = (\lambda/4\pi)(d_{\boldsymbol{b}_B \boldsymbol{r}_R}^{[m]} + d_{\boldsymbol{r}_R \boldsymbol{u}_U}^{[m]})^{-1}$. For the m^{th} RIS, the complex channel coefficients is specified by $\beta^{[m]}$. The delay between the BS and the r^{th} element on the m^{th} RIS is specified as $\tau_{\boldsymbol{b}_B \boldsymbol{r}_r}^{[m]} = d_{\boldsymbol{b}_B \boldsymbol{r}_r}^{[m]}/c$. Likewise in the m^{th} RIS-UE link, the delay from the r^{th} element on the m^{th} RIS to the u^{th} UE antenna is specified as $\tau_{\boldsymbol{r}_r \boldsymbol{u}_u}^{[m]} = d_{\boldsymbol{r}_r \boldsymbol{u}_u}^{[m]}/c$. The reflection coefficients of the m^{th} RIS during the t^{th} OFDM symbol can be decomposed into $\boldsymbol{\Omega}_t^{[m]} = \gamma_t^{[m]} \boldsymbol{\Gamma}^{[m]}$ where $\gamma_t^{[m]}$ is a complex scalar value, $\boldsymbol{\Gamma}^{[m]} = \mathrm{diag}(e^{j\vartheta_1^{[m]}}, e^{j\vartheta_2^{[m]}}, \cdots, e^{j\vartheta_{N_R}^{[m]}})$ is a diagonal matrix, and $\vartheta_r^{[m]}$ is the phase of the r^{th} element of the m^{th} RIS.

Assumption 1. *Misorientation changes at a rate far slower than the T OFDM symbols. Further, the channel is assumed constant during the transmission and reception of T OFDM symbols. The value of T is on the order of the inverse of the bandwidth.*

B. Compact Near-Field Signal Representations

Using Assumption 1, the time t is dropped from the channel matrices and the useful part of the received signal at the u^{th} UE antenna is

$$\mu_{t,u}[n] = \sum_{m=1}^{M_1} \gamma_t^{[m]} \beta^{[m]} \boldsymbol{a}^{[m]\mathrm{T}}(\boldsymbol{u}_u) \boldsymbol{\Gamma}^{[m]} \boldsymbol{a}^{[m]}(\boldsymbol{b}_B) x[n], \tag{3}$$

where $\boldsymbol{a}^{[m]}(\boldsymbol{u}_u) = [e^{-j2\pi f_n \tau_{\boldsymbol{r}_1 \boldsymbol{u}_u}^{[m]}}, \cdots, e^{-j2\pi f_n \tau_{\boldsymbol{r}_{N_R^{[m]}} \boldsymbol{u}_u}^{[m]}}]^{\mathrm{T}}$ and $\boldsymbol{a}^{[m]}(\boldsymbol{b}_B) = [e^{-j2\pi f_n \tau_{\boldsymbol{b}_B \boldsymbol{r}_1}^{[m]}}, \cdots, e^{-j2\pi f_n \tau_{\boldsymbol{b}_B \boldsymbol{r}_{N_R^{[m]}}}^{[m]}}]^{\mathrm{T}}$.

C. Far-Field Signal Representations

To analyze the information available in the far-field and the near-field, we present the far-field approximation of the useful part of the signal received in the near-field propagation regime. The far field model (with a different parameterization that the

model in [14]) of the useful part of the received signal can be obtained from (2) and expressed as

$$\begin{aligned}&\boldsymbol{\mu}_t[n] = \\ &\sum_{m=1}^{M_1} \gamma_t^{[m]} \beta^{[m]} \rho^{[m]} \boldsymbol{a}_{UR}(\Delta_{\boldsymbol{r}_R \boldsymbol{u}_U}^{[m]}) \boldsymbol{a}_{RU}^{\mathrm{H}}(\Delta_{\boldsymbol{r}_R \boldsymbol{u}_U}^{[m]}) \boldsymbol{\Gamma}^{[m]} \\ &\times \boldsymbol{a}_{RB}(\Delta_{\boldsymbol{b}_B \boldsymbol{r}_R}^{[m]}) x[n] e^{-j2\pi f_n (\tau_{\boldsymbol{b}_B \boldsymbol{r}_R}^{[m]} + \tau_{\boldsymbol{r}_R \boldsymbol{u}_U}^{[m]})},\end{aligned} \tag{4}$$

where the array responses between the G^{th} entity and the V^{th} entity as $\boldsymbol{a}_{GV}(\Delta_{\boldsymbol{g}_G \boldsymbol{v}_V}) = e^{-j2\frac{\pi}{\lambda_n}\Delta_{\boldsymbol{g}_G \boldsymbol{v}_V}^{\mathrm{T}} \boldsymbol{s}_g}$, $\boldsymbol{a}_{VG}(\Delta_{\boldsymbol{g}_G \boldsymbol{v}_V}) = e^{-j2\frac{\pi}{\lambda_n}\Delta_{\boldsymbol{g}_G \boldsymbol{v}_V}^{\mathrm{T}} \boldsymbol{s}_v}$.

III. Available Information in the Received Signal

In this section, we present bounds on the information available from the received signals.

A. Error Bounds on Parameters

The analysis in this work is based both on the received signal specified by (2) and some of the parameters present in this signal. The state of these parameters is an indicator of the performance of both communication and localization systems; hence, in this section, we more clearly highlight these parameters. The RIS related channel parameters are $\boldsymbol{\theta}_{\boldsymbol{r}_R \boldsymbol{u}_U} \triangleq \left[\theta_{\boldsymbol{r}_R \boldsymbol{u}_U}^{[1]}, \cdots, \theta_{\boldsymbol{r}_R \boldsymbol{u}_U}^{[M_1]}\right]^{\mathrm{T}}, \boldsymbol{\phi}_{\boldsymbol{r}_R \boldsymbol{u}_U} \triangleq \left[\phi_{\boldsymbol{r}_R \boldsymbol{u}_U}^{[1]}, \cdots, \phi_{\boldsymbol{r}_R \boldsymbol{u}_U}^{[M_1]}\right]^{\mathrm{T}}, \boldsymbol{\tau}_{\boldsymbol{r}_R \boldsymbol{u}_U} \triangleq \left[\tau_{\boldsymbol{r}_R \boldsymbol{u}_U}^{[1]}, \cdots, \tau_{\boldsymbol{r}_R \boldsymbol{u}_U}^{[M_1]}\right]^{\mathrm{T}}$, $\boldsymbol{\beta} \triangleq \left[\beta^{[1]}, \ldots, \beta^{[M_1]}\right]^{\mathrm{T}}, \boldsymbol{\Phi}_R \triangleq \left[\boldsymbol{\Phi}_R^{[1]\mathrm{T}}, \ldots, \boldsymbol{\Phi}_R^{[M_1]\mathrm{T}}\right]^{\mathrm{T}}$, and these unknown channel parameters related to RIS can be represented by the vector

$$\boldsymbol{\eta} \triangleq \left[\boldsymbol{\Phi}_R^{\mathrm{T}}, \boldsymbol{\theta}_{\boldsymbol{r}_R \boldsymbol{u}_U}^{\mathrm{T}}, \boldsymbol{\phi}_{\boldsymbol{r}_R \boldsymbol{u}_U}^{\mathrm{T}}, \boldsymbol{\tau}_{\boldsymbol{r}_R \boldsymbol{u}_U}^{\mathrm{T}}, \boldsymbol{\beta}_{\mathrm{R}}^{\mathrm{T}}, \boldsymbol{\beta}_{\mathrm{I}}^{\mathrm{T}}\right]^{\mathrm{T}}, \tag{5}$$

where $\boldsymbol{\beta}_{\mathrm{R}} \triangleq \Re\{\boldsymbol{\beta}\}$, and $\boldsymbol{\beta}_{\mathrm{I}} \triangleq \Im\{\boldsymbol{\beta}\}$ are the real and imaginary parts of $\boldsymbol{\beta}$, respectively. Now, we define the geometric channel parameters $\boldsymbol{\eta}_1 \triangleq \left[\boldsymbol{\Phi}_R^{\mathrm{T}}, \boldsymbol{\theta}_{\boldsymbol{r}_R \boldsymbol{u}_U}^{\mathrm{T}}, \boldsymbol{\phi}_{\boldsymbol{r}_R \boldsymbol{u}_U}^{\mathrm{T}}, \boldsymbol{\tau}_{\boldsymbol{r}_R \boldsymbol{u}_U}^{\mathrm{T}}, \boldsymbol{\Phi}_U^{\mathrm{T}}\right]^{\mathrm{T}}$ and the nuisance parameters as $\boldsymbol{\eta}_2 \triangleq \left[\boldsymbol{\beta}_{\mathrm{R}}^{\mathrm{T}}, \boldsymbol{\beta}_{\mathrm{I}}^{\mathrm{T}}\right]^{\mathrm{T}}$, hence, $\boldsymbol{\eta} \triangleq \left[\boldsymbol{\eta}_1^{\mathrm{T}}, \boldsymbol{\eta}_2^{\mathrm{T}}\right]^{\mathrm{T}}$. An alternative representation according to the parameters associated with the m^{th} RIS path is $\boldsymbol{\eta}^{[m]} \triangleq \left[\boldsymbol{\Phi}_R^{[m]\mathrm{T}}, \theta_{\boldsymbol{r}_R \boldsymbol{u}_U}^{[m]}, \phi_{\boldsymbol{r}_R \boldsymbol{u}_U}^{[m]}, \tau_{\boldsymbol{r}_R \boldsymbol{u}_U}^{[m]}, \boldsymbol{\Phi}_U^{\mathrm{T}}, \beta_{\mathrm{R}}^{[m]}, \beta_{\mathrm{I}}^{[m]}\right]^{\mathrm{T}}$, and $\boldsymbol{\eta}$ is defined as $\boldsymbol{\eta} \triangleq \left[\boldsymbol{\eta}^{[1]\mathrm{T}}, \boldsymbol{\eta}^{[2]\mathrm{T}}, \cdots, \boldsymbol{\eta}^{[M_1]\mathrm{T}}\right]^{\mathrm{T}}$, where the parameters associated with the m^{th} RIS path can also be divided into the geometric channel parameters, $\boldsymbol{\eta}_1^{[m]}$, and the nuisance parameters, $\boldsymbol{\eta}_2^{[m]}$, such that $\boldsymbol{\eta}^{[m]} \triangleq \left[\boldsymbol{\eta}_1^{[m]\mathrm{T}}, \boldsymbol{\eta}_2^{[m]\mathrm{T}}\right]^{\mathrm{T}}$.

Remark 1. *The parameterization of channel parameters discussed in this section has implicitly assumed that the BS is perfectly located i.e., $\boldsymbol{p}_B = \tilde{\boldsymbol{p}}_B$. It should be noted that $\boldsymbol{\Phi}_U$ is not dependent on any RIS. The parameter $\boldsymbol{\Phi}_U$ is placed in the parameter vector of the m^{th} RIS only for notational simplicity. Henceforth, the BS is assumed perfectly located, and it is considered to serve as the global origin.*

B. Mathematical Preliminaries

Here, we present mathematical preliminaries needed to derive bounds for both deterministic and random channel parameters. We note that the error covariance matrix of an unbiased estimator, $\hat{\boldsymbol{\eta}}$, satisfies the following information inequality $\mathbb{E}_{\boldsymbol{y};\boldsymbol{\eta}}\left\{(\hat{\boldsymbol{\eta}} - \boldsymbol{\eta})(\hat{\boldsymbol{\eta}} - \boldsymbol{\eta})^{\mathrm{T}}\right\} \succeq \mathbf{J}_{\boldsymbol{y};\boldsymbol{\eta}}^{-1}$, where $\mathbf{J}_{\boldsymbol{y};\boldsymbol{\eta}}$ is the general FIM for the parameter vector $\boldsymbol{\eta}$.

Definition 1. *The general FIM for a parameter vector, $\boldsymbol{\eta}$, defined as $\mathbf{J}_{\boldsymbol{y};\boldsymbol{\eta}} = \boldsymbol{F}_{\boldsymbol{y};\boldsymbol{\eta}}(\boldsymbol{y};\boldsymbol{\eta},\boldsymbol{\eta},\boldsymbol{\eta})$ is the summation of the FIM obtained from the likelihood due to the observations defined as $\mathbf{J}_{\boldsymbol{y}|\boldsymbol{\eta}} = \boldsymbol{F}_{\boldsymbol{y}}(\boldsymbol{y}|\boldsymbol{\eta};\boldsymbol{\eta},\boldsymbol{\eta})$ and the FIM from* a priori *information about the parameter vector defined as $\mathbf{J}_{\boldsymbol{\eta}} = \boldsymbol{F}_{\boldsymbol{\eta}}(\boldsymbol{\eta};\boldsymbol{\eta},\boldsymbol{\eta})$. In mathematical terms, we have*

$$\begin{aligned}\mathbf{J}_{\boldsymbol{y};\boldsymbol{\eta}} &\triangleq \mathbb{E}_{\boldsymbol{y};\boldsymbol{\eta}}\left[-\frac{\partial^2 \ln \chi(\boldsymbol{y};\boldsymbol{\eta})}{\partial \boldsymbol{\eta} \partial \boldsymbol{\eta}^{\mathrm{T}}}\right] \\ &= -\mathbb{E}_{\boldsymbol{y}}\left[\frac{\partial^2 \ln \chi(\boldsymbol{y}|\boldsymbol{\eta})}{\partial \boldsymbol{\eta} \partial \boldsymbol{\eta}^{\mathrm{T}}}\right] - \mathbb{E}_{\boldsymbol{\eta}}\left[\frac{\partial^2 \ln \chi(\boldsymbol{\eta})}{\partial \boldsymbol{\eta} \partial \boldsymbol{\eta}^{\mathrm{T}}}\right] = \mathbf{J}_{\boldsymbol{y}|\boldsymbol{\eta}} + \mathbf{J}_{\boldsymbol{\eta}},\end{aligned} \tag{6}$$

where $\chi(\boldsymbol{y};\boldsymbol{\eta})$ denotes the probability density function (PDF) of $\boldsymbol{y}$ and $\boldsymbol{\eta}$.

The number of elements in the Fisher information matrix increases quadratically with an increase in the number of parameters; hence, due to the potentially large dimensions of the Fisher information matrix, it is beneficial to focus on the partition corresponding to the parameters of interest. The Schur's complement [15] provides a method of achieving this partition and the resulting partition is the EFIM.

Definition 2. *Given a parameter vector, $\boldsymbol{\eta} \triangleq \left[\boldsymbol{\eta}_1^{\mathrm{T}}, \boldsymbol{\eta}_2^{\mathrm{T}}\right]^{\mathrm{T}}$, where $\boldsymbol{\eta}_1$ is the parameter of interest, the resultant FIM has the structure*

$$\mathbf{J}_{\boldsymbol{y};\boldsymbol{\eta}} = \begin{bmatrix} \mathbf{J}_{\boldsymbol{y};\boldsymbol{\eta}_1} & \mathbf{J}_{\boldsymbol{y};\boldsymbol{\eta}_1,\boldsymbol{\eta}_2} \\ \mathbf{J}_{\boldsymbol{y};\boldsymbol{\eta}_1,\boldsymbol{\eta}_2}^{\mathrm{T}} & \mathbf{J}_{\boldsymbol{y};\boldsymbol{\eta}_2} \end{bmatrix},$$

where $\boldsymbol{\eta} \in \mathbb{R}^N, \boldsymbol{\eta}_1 \in \mathbb{R}^n, \mathbf{J}_{\boldsymbol{y};\boldsymbol{\eta}_1} \in \mathbb{R}^{n \times n}, \mathbf{J}_{\boldsymbol{y};\boldsymbol{\eta}_1,\boldsymbol{\eta}_2} \in \mathbb{R}^{n \times (N-n)}$, and $\mathbf{J}_{\boldsymbol{y};\boldsymbol{\eta}_2} \in \mathbb{R}^{(N-n)\times(N-n)}$ with $n < N$, and the EFIM [16] of parameter $\boldsymbol{\eta}_1$ is given by

$$\mathbf{J}_{\boldsymbol{y};\boldsymbol{\eta}_1}^{\mathrm{e}} = \mathbf{J}_{\boldsymbol{y};\boldsymbol{\eta}_1} - \mathbf{J}_{\boldsymbol{y};\boldsymbol{\eta}_1}^{nu} = \mathbf{J}_{\boldsymbol{y};\boldsymbol{\eta}_1} - \mathbf{J}_{\boldsymbol{y};\boldsymbol{\eta}_1,\boldsymbol{\eta}_2} \mathbf{J}_{\boldsymbol{y};\boldsymbol{\eta}_2}^{-1} \mathbf{J}_{\boldsymbol{y};\boldsymbol{\eta}_1,\boldsymbol{\eta}_2}^{\mathrm{T}}. \tag{7}$$

This EFIM captures all the required information about the parameters of interest present in the FIM; as observed from the relation $(\mathbf{J}_{\boldsymbol{y};\boldsymbol{\eta}_1}^{\mathrm{e}})^{-1} = [\mathbf{J}_{\boldsymbol{y};\boldsymbol{\eta}}^{-1}]_{[1:n,1:n]}$.

Definition 3. *The parameter vector, $\boldsymbol{\eta}$, is estimatable iff the general FIM, $\mathbf{J}_{\boldsymbol{y};\boldsymbol{\eta}} \succ 0$.*

Proposition 1. *Defining a parameter vector $\boldsymbol{\eta} = \left[\boldsymbol{\eta}_1^{\mathrm{T}}, \eta_{N_\eta}\right]^{\mathrm{T}} = [\eta_1, \eta_2, \cdots, \eta_{N_{\eta-1}}, \eta_{N_\eta}]^{\mathrm{T}}$, where $\boldsymbol{\eta}_1$ is the parameter of interest and η_{N_η} is a nuisance parameter. For a subset of the parameter vector, $\tilde{\boldsymbol{\eta}} = [\eta_v, \eta_{N_\eta}]^{\mathrm{T}}$ where $v \in \{1, 2, \cdots, N_{\eta-1}\}$; if the resultant EFIM, $\mathrm{J}_{\boldsymbol{y};\tilde{\boldsymbol{\eta}}}^{\mathrm{e}} = 0$, then the EFIM, $\mathbf{J}_{\boldsymbol{y};\boldsymbol{\eta}_1}^{\mathrm{e}} \not\succ 0$.*

Proof. See Appendix A. □

C. Fisher Information Matrix for Channel Parameters

To derive the FIM for the channel parameters from the received signals, we consider the t^{th} OFDM transmission with N subcarriers, and the likelihood expression conditioned on the parameter vector, $\boldsymbol{\eta}$, is[1] $\chi(\boldsymbol{y}_t[n]|\boldsymbol{\eta}) \propto \exp\left\{\frac{2}{N_0}\sum_{n=1}^{N}\Re\left\{\boldsymbol{\mu}_t^{\mathrm{H}}[n]\boldsymbol{y}_t[n]\right\} - \frac{1}{N_0}\sum_{n=1}^{N}\|\boldsymbol{\mu}_t[n]\|_2^2\right\}$. The FIM from observations, $\mathbf{J}_{\boldsymbol{y}|\boldsymbol{\eta}}$, of the random vector, $\boldsymbol{y}$, is obtained by substituting $\chi(\boldsymbol{y}_t[n]|\boldsymbol{\eta})$ into (6) in Definition 1. The *a priori* information about channel parameters and RIS orientation is incorporated through the likelihood which is expressed as $\chi(\boldsymbol{\eta}) = \prod_{m=1}^{M_1}\chi(\boldsymbol{\eta}^{[m]}|\boldsymbol{p}_R^{[m]}, \boldsymbol{p}_U)$. The equation above assumes that there is independence between channel parameters from distinct RISs. Furthermore, we assume that the UE orientation is independent of the orientation of the RISs and the parameters in each distinct path are independent of each other. The Fisher information matrix from *a priori* information is $\mathbf{J}_{\boldsymbol{\eta}} = \operatorname{diag}\left[\boldsymbol{\Xi}_{\boldsymbol{\eta}^{[1]},\boldsymbol{\eta}^{[1]}}^{\boldsymbol{\eta}^{[1]}}, \cdots, \boldsymbol{\Xi}_{\boldsymbol{\eta}^{[M_1]},\boldsymbol{\eta}^{[M_1]}}^{\boldsymbol{\eta}^{[M_1]}}\right]$, where the FIM from the *a priori* information related to the likelihood $\chi(\boldsymbol{\eta}^{[m]}|\boldsymbol{p}_R^{[m]}, \boldsymbol{p}_U)$ is $\boldsymbol{\Xi}_{\boldsymbol{\eta}^{[m]},\boldsymbol{\eta}^{[m]}}^{\boldsymbol{\eta}^{[m]}} = \boldsymbol{F}_{\boldsymbol{\eta}}(\boldsymbol{\eta}^{[m]}|\boldsymbol{p}_R^{[m]}, \boldsymbol{p}_U; \boldsymbol{\eta}^{[m]}, \boldsymbol{\eta}^{[m]})$. Note that $\boldsymbol{\Xi}_{\boldsymbol{\eta}^{[m]},\boldsymbol{\eta}^{[m]}}^{\boldsymbol{\eta}^{[m]}}, m \in \{1, \cdots, M_1\}$ are diagonal matrices as the parameters in each path are assumed to be independent from each other. The general FIM is obtained from $\mathbf{J}_{\boldsymbol{y}|\boldsymbol{\eta}}$ and $\mathbf{J}_{\boldsymbol{\eta}}$ according to Definition 1. The FIM $\mathbf{J}_{\boldsymbol{y}|\boldsymbol{\eta}}$ of the channel parameters specified by (5) has $(M_1+1)^2$ submatrices, and these submatrices are obtained using

$$[\mathbf{J}_{\boldsymbol{y}|\boldsymbol{\eta}}]_{[v,g]} = \frac{2}{N_0}\sum_{u=1}^{N_U}\sum_{n=1}^{N}\sum_{t=1}^{T}\Re\left\{\nabla_{[\boldsymbol{\eta}]_{[v]}}^{\mathrm{H}}\mu_{t,u}[n]\nabla_{[\boldsymbol{\eta}]_{[g]}}\mu_{t,u}[n]\right\}, \tag{8}$$

Note that the FIM obtained is challenging to analyze. Hence, we make some assumptions for tractability in the presentation of the necessary conditions for estimating both deterministic and random channel parameters.

Assumption 2. *The degrees of freedom provided by the T OFDM symbols are used to impose the following constraints $\sum_{t=1}^{T}\gamma_t^{[m]} = 0$, $\sum_{t=1}^{T}\gamma_t^{[m]\mathrm{H}}\gamma_t^{[m]} = 1$, $\forall\ m$, and $\sum_{t=1}^{T}\gamma_t^{[m_1]\mathrm{H}}\gamma_t^{[m_2]} = 0$, $\forall\ m_1 \neq m_2$. These constraints make the distinct RIS paths separable, resulting in the block diagonalization of the FIM from the observations, $\mathbf{J}_{\boldsymbol{y}|\boldsymbol{\eta}}$. This block diagonalization helps analyze the information provided by each RIS path.*

Assumption 2 is used to ensure the diagonalization of the FIM. With this diagonalization, the general FIM obtained from $\mathbf{J}_{\boldsymbol{y}|\boldsymbol{\eta}}$ and $\mathbf{J}_{\boldsymbol{\eta}}$ according to Definition 1 is also a diagonal matrix $\mathbf{J}_{\boldsymbol{y};\boldsymbol{\eta}} = \operatorname{diag}\left[\mathbf{J}_{\boldsymbol{y};\boldsymbol{\eta}^{[1]}}, \cdots, \mathbf{J}_{\boldsymbol{y};\boldsymbol{\eta}^{[M_1]}}\right]$. With Definition 3 and the block diagonal nature of the general Fisher information matrix (FIM), $\mathbf{J}_{\boldsymbol{y};\boldsymbol{\eta}}$, it is sufficient to determine estimatability of a parameter vector, $\boldsymbol{\eta}$, by establishing the positive definiteness of all the diagonal entries in $\mathbf{J}_{\boldsymbol{y};\boldsymbol{\eta}}$. However, not all parameters are useful, hence a more efficient metric is the general EFIM $\mathbf{J}_{\boldsymbol{y};\boldsymbol{\eta}_1}^{\mathrm{e}} = \operatorname{diag}\left[\mathbf{J}_{\boldsymbol{y};\boldsymbol{\eta}_1^{[1]}}^{\mathrm{e}}, \cdots, \mathbf{J}_{\boldsymbol{y};\boldsymbol{\eta}_1^{[M_1]}}^{\mathrm{e}}\right]$. The term $\mathbf{J}_{\boldsymbol{y};\boldsymbol{\eta}_1^{[m]}}^{\mathrm{e}}$, is the general EFIM of the m^{th} path derived based on the vector of parameters of interest $\boldsymbol{\eta}_1^{[m]}$[2].

D. Fisher Information for the RIS Parameters

The RIS paths have identical channel parameters. Hence it suffices to analyze a single RIS path. Therefore, we apply Assumption 2 and investigate the estimatability of the geometric channel parameters related to the m^{th} RIS.

Lemma 1. *In the far-field, the vector of geometric channel parameters is not estimatatible at the UE without* a priori *information about the orientation of the RIS or* a priori *information about the channel complex path gains.*

Proof. See Appendix B. □

Lemma 2. *In the near-field, the vector of geometric channel parameters is not estimatatible at the UE without* a priori *information about the channel complex path gains if there is also no* a priori *information about the orientation of the RIS and if $N_U < 2$.*

Proof. See Appendix C. □

Combining the results of Lemmas 1 and 2, we are now ready to state the main result of this paper in the following Theorem.

Theorem 1. *In the far-field, the estimation and correction of RIS orientation offset based on the received signals at the UE is not possible due to the absence of* a priori *information about the channel's complex path gains. However, in the near-field, this correction of RIS orientation offset is not hindered by the absence of* a priori *information about the channel complex path gains when $N_U > 1$.*

Remark 2. *The complex path gain can be normalized through the SNR to reduce from a complex path gain to an unknown phase offset term. Hence, we can restate the above Lemmas and Theorem, focusing only on the* a priori *information about the unknown phase offset. Because quantifying* a priori *information about this unknown phase offset is virtually impossible, Theorem 1 practically implies the possibility of estimating and correcting an RIS orientation offset only exists in the near-field.*

IV. Numerical Results

This section uses Monte-Carlo simulations to verify that the possibility of a UE estimating the RIS orientation offset exists in the near field but not in the far field. The system setup includes a single perfectly located BS whose centroid is also the global origin of the coordinate system i.e., $\boldsymbol{p}_B = [0,0,0]^{\mathrm{T}} = \tilde{\boldsymbol{p}}_B$ and $\boldsymbol{Q}_B = \boldsymbol{I}$. All position vectors are in meters, and all orientation vectors are in radians. The system setup includes two RISs that reflect the transmitted signal to the UE. The first RIS is misoriented with its centroid

[1]The likelihood is easily expressible in scalar terms by considering the signal at each receive antenna as independent observations.

[2]Definition 3 is easily extended to define necessary and sufficient conditions for the estimatability of the parameter of interest, $\boldsymbol{\eta}_1^{[m]}$ based on the EFIM.

located at $\boldsymbol{p}_R^{[1]} = \tilde{\boldsymbol{p}}_R^{[1]} = [10, 8, 4]^{\mathrm{T}}$ with the following rotation angles $\boldsymbol{\Phi}_R^{[1]} = [0.1, 0.2, 0.1]^{\mathrm{T}}$, while the other RIS is perfectly located at $\boldsymbol{p}_R^{[2]} = \tilde{\boldsymbol{p}}_R^{[2]} = [10, 8.5, 4]^{\mathrm{T}}$ and $Q_R^{[2]} = \boldsymbol{I}$. The UE location is described with $\boldsymbol{p}_U = \tilde{\boldsymbol{p}}_U = [12, 10, 3]^{\mathrm{T}}$ and $\boldsymbol{Q}_U = \boldsymbol{I}$. The second RIS has been used to localize the UE. Subsequently, the UE attempts to correct the RIS orientation offset of the first RIS. Hence, we have the parameter vector $\boldsymbol{\eta}^{[1]} \triangleq \left[\boldsymbol{\Phi}_R^{[1]\mathrm{T}}, \theta^{[1]}_{\boldsymbol{r}_R \boldsymbol{u}_U}, \phi^{[1]}_{\boldsymbol{r}_R \boldsymbol{u}_U}, \beta_{\mathrm{R}}^{[1]}, \beta_{\mathrm{I}}^{[1]}\right]^{\mathrm{T}}$. The considered wavelength is $\lambda = 3$ cm with the elements in each RIS spaced by 1.5 cm. There are $N = 256$ subcarriers, a single antenna at the BS and no transmit beamforming, the transmit power is 23 dBm, the noise power spectral density (PSD) is $N_0 = -174$ dBm/Hz, and the antenna gains of the transmit and receive antennas are set to $G_B = G_U = 2$ dB, respectively. We combine the pathloss and the noise power into a composite noise power, σ^2. We define the SNR as P/σ^2, where P is the product of the transmit power, transmit, and receive antenna gains. We focus on the case with uniform rectangular arrays (URAs) at the BS, RIS, and the UE with their respective normal vectors originally pointing in the z direction. At the considered UE position and with the Fraunhofer distance defined in [17], the UE is in the near-field of the first RIS when $N_R^{[1]} \geq 100$ and in the near-field of the second RIS when $N_R^{[2]} \geq 90$.

The UE attempts to use either the *correct* near-field model (3) or the *incorrect* far-field model (4) to correct the orientation offset of the first RIS. Hence, the OEB of the orientation offset of the first RIS is plotted. In all applicable plots, the prefix "FF" is used to distinguish the *incorrect* case where a far-field model is applied to this near-field simulation setup from the *correct* case where the near-field model is used for the near-field setup. There is no *a priori* information about the complex path gains, and the *a priori* information about the orientation offset is quantified as a fraction of the SNR, P/σ^2. In Fig. 2a, when the near-field model is used, the OEB is shown to decrease with an increase in the number of receive antennas; however, when the far-field model is used, the OEB stays relatively constant for a varying number of receive antennas. While using the near-field model, the OEB is prohibitively large when N_U is small, especially for a small RIS. More specifically, when N_U is small, and there is little or no *a priori* information, the resulting EFIM, $\mathbf{J}^{\mathrm{e}}_{\boldsymbol{y};\boldsymbol{\eta}_1^{[1]}}$, is sometimes almost singular; hence $\mathbf{J}^{\mathrm{e}}_{\boldsymbol{y};\boldsymbol{\eta}_1^{[1]}}$ has a relatively small eigenvalue. This is confirmed in Fig. 2b, which presents the smallest eigenvalue ($\lambda^{\mathrm{e}}_{min}$) of $\mathbf{J}^{\mathrm{e}}_{\boldsymbol{y};\boldsymbol{\eta}_1^{[1]}}$ as a function of N_U. In Fig. 2b, while using the near-field model, the smallest eigenvalue increases significantly with an increase in N_U, when using the far-field model, the smallest eigenvalue stays relatively constant irrespective of N_U. This observation validates Lemmas 1 and 2. More specifically, it validates that in the far-field, the OEB is independent of N_U and only depends on the *a priori* information.

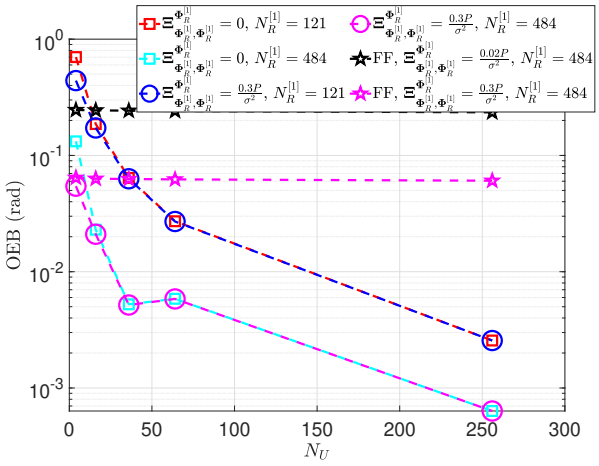

(a)

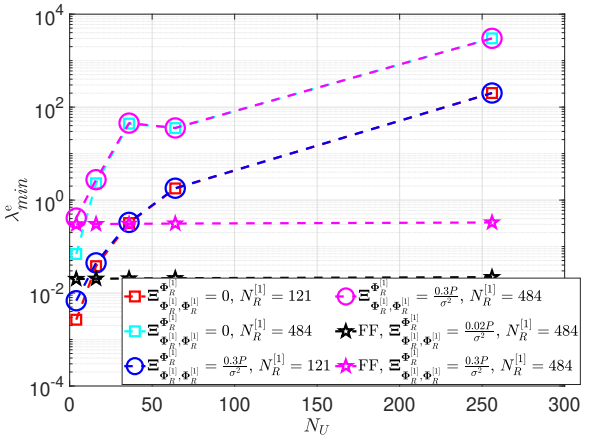

(b)

Fig. 2. (a) OEB of the orientation offset of the first RIS vs. the number of receive antennas. (b) $\lambda^{\mathrm{e}}_{min}$ vs. N_U is plotted with $\lambda^{\mathrm{e}}_{min}$ normalized by the SNR. Plot (b) investigates the direct relationship between the RIS orientation offset and the complex path gain by presenting the smallest eigenvalue of the EFIM for the channel parameters when the only unknown channel parameters are the RIS orientation offset and the complex path gain. In both plots, we also consider varying amounts of *a priori* information, and a varying number of elements on the first RIS, i.e., $N_R^{[1]}$.

V. Conclusion

In this work, we considered the downlink of a SIMO system operating with OFDM with one or more RISs providing reflected signals to a UE under both near-field and far-field propagation regimes. We showed through the EFIM for channel parameters that an unknown phase offset in the received signal at the UE makes it impossible to estimate and correct any RIS orientation offset through these received signals in the far-field. However, in the near-field, an unknown phase offset in the received signal at the UE does not hinder the estimation of the RIS orientation offset when there is more than one receive antenna. This non-trivial result indicates that the possibility of correcting an RIS orientation offset through the received signals at the UE only exists while the UE is in the near-field.

APPENDIX

A. Proof of Proposition 1

In general, an $N_\eta \times N_\eta$ symmetric matrix, $\mathbf{J}$ is positive definite, if $\boldsymbol{v}^{\mathrm{T}}\mathbf{J}\boldsymbol{v} > 0$, for all non-zero $\boldsymbol{v} \in \mathbb{C}^{N_\eta \times 1}$. Now, suppose a zero lies on the diagonal of $\mathbf{J}$ such that $[\mathbf{J}]_{[n,n]} = 0$ and suppose we select a vector $\boldsymbol{v}$ with all zero entries except at its n^{th} entry. With this selection, we have $\boldsymbol{v}^{\mathrm{T}}\mathbf{J}\boldsymbol{v} = [\boldsymbol{v}]_{[n]}^{\mathrm{T}}[\mathbf{J}]_{[n,n]}[\boldsymbol{v}]_{[n]} = 0$ and by definition, $\mathbf{J} \not\succ 0$. The proof is complete.

B. Proof of Lemma 1

See Appendix D in [1].

C. Proof of Lemma 2

This proof is concerned with the m^{th} RIS path, hence the superscript $(\cdot)^{[m]}$ is dropped when notationally convenient. It suffices to show that the EFIM of a parameter vector, $\tilde{\boldsymbol{\eta}}^{[m]} = [\boldsymbol{\Phi}_R^{[m]}, \beta^{[m]}]$ is zero. After obtaining the first derivatives, the general FIM is

$$\mathbf{J}_{\boldsymbol{y};\tilde{\boldsymbol{\eta}}^{[m]}} = \begin{bmatrix} \mathbf{J}_{\boldsymbol{y}|\boldsymbol{\Phi}_R} + \boldsymbol{\Xi}_{\boldsymbol{\Phi}_R,\boldsymbol{\Phi}_R}^{\boldsymbol{\Phi}_R} & \mathbf{J}_{\boldsymbol{y}|\boldsymbol{\Phi}_R,\beta_R} & \mathbf{J}_{\boldsymbol{y}|\boldsymbol{\Phi}_R,\beta_I} \\ \mathbf{J}_{\boldsymbol{y}|\boldsymbol{\Phi}_R,\beta_R}^{\mathrm{T}} & \mathbf{J}_{\boldsymbol{y}|\beta_R} + \boldsymbol{\Xi}_{\beta_R,\beta_R}^{\beta_R} & 0 \\ \mathbf{J}_{\boldsymbol{y}|\boldsymbol{\Phi}_R,\beta_I}^{\mathrm{T}} & 0 & \mathbf{J}_{\boldsymbol{y}|\beta_I} + \boldsymbol{\Xi}_{\beta_R,\beta_R}^{\beta_R} \end{bmatrix}. \tag{9}$$

Defining the following vector $\boldsymbol{K}(\boldsymbol{g}_g) = \text{diag}\left[\nabla_{\boldsymbol{\Phi}_R}\tau_{\boldsymbol{r}_1}\boldsymbol{g}_g, \nabla_{\boldsymbol{\Phi}_R}\tau_{\boldsymbol{r}_2}\boldsymbol{g}_g, \cdots, \nabla_{\boldsymbol{\Phi}_R}\tau_{\boldsymbol{r}_{N_R}}\boldsymbol{g}_g\right]$, the FIMs from observations are written as

$$\mathbf{J}_{\boldsymbol{y}|\boldsymbol{\Phi}_R} = 2/N_0(2\pi f_c)^2 \sum_{n=1}^{N} |x[n]|^2 |\beta^{[m]}|^2 \times \sum_{u=1}^{N_U} \Re\left\{ \boldsymbol{a}^{\mathrm{H}}(\boldsymbol{b}_B)\left[\boldsymbol{\Gamma}^{[m]\mathrm{H}}\boldsymbol{K}^*(\boldsymbol{u}_u) + \boldsymbol{K}^{\mathrm{H}}(\boldsymbol{b}_B)\boldsymbol{\Gamma}^{[m]\mathrm{H}}\right]\boldsymbol{a}(\boldsymbol{u}_u) \boldsymbol{a}^{\mathrm{T}}(\boldsymbol{u}_u)\left[\boldsymbol{K}^{\mathrm{T}}(\boldsymbol{u}_u)\boldsymbol{\Gamma}^{[m]} + \boldsymbol{\Gamma}^{[m]}\boldsymbol{K}(\boldsymbol{b}_B)\right]\boldsymbol{a}(\boldsymbol{b}_B)\right\}, \tag{10}$$

$$\mathbf{J}_{\boldsymbol{y}|\boldsymbol{\Phi}_R,\beta_R} = 2/N_0(2\pi f_c) \sum_{n=1}^{N} |x[n]|^2 \times \sum_{u=1}^{N_U} \Re\left\{ j\beta^{[m]\mathrm{H}}\boldsymbol{a}^{\mathrm{H}}(\boldsymbol{b}_B)\left[\boldsymbol{\Gamma}^{[m]\mathrm{H}}\boldsymbol{K}^*(\boldsymbol{u}_u) + \boldsymbol{K}^{\mathrm{H}}(\boldsymbol{b}_B)\boldsymbol{\Gamma}^{[m]\mathrm{H}}\right]\times \boldsymbol{a}(\boldsymbol{u}_u)\boldsymbol{a}^{\mathrm{T}}(\boldsymbol{u}_u)\boldsymbol{\Gamma}^{[m]}\boldsymbol{a}(\boldsymbol{b}_B)\right\}, \tag{11}$$

$$\mathbf{J}_{\boldsymbol{y}|\boldsymbol{\Phi}_R,\beta_I} = -2/N_0(2\pi f_c) \sum_{n=1}^{N} |x[n]|^2 \times \sum_{u=1}^{N_U} \Re\left\{ \beta^{[m]\mathrm{H}}\boldsymbol{a}^{\mathrm{H}}(\boldsymbol{b}_B)\left[\boldsymbol{\Gamma}^{[m]\mathrm{H}}\boldsymbol{K}^*(\boldsymbol{u}_u) + \boldsymbol{K}^{\mathrm{H}}(\boldsymbol{b}_B)\boldsymbol{\Gamma}^{[m]\mathrm{H}}\right]\times \boldsymbol{a}(\boldsymbol{u}_u)\boldsymbol{a}^{\mathrm{T}}(\boldsymbol{u}_u)\boldsymbol{\Gamma}^{[m]}\boldsymbol{a}(\boldsymbol{b}_B)\right\}, \tag{12}$$

$\mathbf{J}_{\boldsymbol{y}|\beta_R} = 2/N_0 \sum_{n=1}^{N} |x[n]|^2 \sum_{u=1}^{N_U} |\boldsymbol{a}^{\mathrm{T}}(\boldsymbol{u}_u)\boldsymbol{\Gamma}^{[m]}\boldsymbol{a}(\boldsymbol{b}_B)|^2$, and the general EFIM is

$$\mathbf{J}^{\mathrm{e}}_{\boldsymbol{y};\tilde{\boldsymbol{\eta}}^{[m]}} = \mathbf{J}_{\boldsymbol{y}|\boldsymbol{\Phi}_R} + \boldsymbol{\Xi}_{\boldsymbol{\Phi}_R,\boldsymbol{\Phi}_R}^{\boldsymbol{\Phi}_R} - [\mathbf{J}_{\boldsymbol{y}|\beta_R} + \boldsymbol{\Xi}_{\beta_R,\beta_R}^{\beta_R}]^{-1} \times [\mathbf{J}_{\boldsymbol{y}|\boldsymbol{\Phi}_R,\beta_R}\mathbf{J}_{\boldsymbol{y}|\boldsymbol{\Phi}_R,\beta_R}^{\mathrm{T}} + \mathbf{J}_{\boldsymbol{y}|\boldsymbol{\Phi}_R,\beta_I}\mathbf{J}_{\boldsymbol{y}|\boldsymbol{\Phi}_R,\beta_I}^{\mathrm{T}}], \tag{13}$$

and with appropriate substitutions, it can be shown that $\mathbf{J}^{\mathrm{e}}_{\boldsymbol{y};\tilde{\boldsymbol{\eta}}^{[m]}} = 0$ when $N_U = 1$, and $\mathbf{J}^{\mathrm{e}}_{\boldsymbol{y};\tilde{\boldsymbol{\eta}}^{[m]}} > 0$ when $N_U > 1$. This proof assumes narrowband transmissions such that $f_c = f_n;\ \forall n$. The proof is complete.

REFERENCES

[1] D.-R. Emenonye, H. S. Dhillon, and R. M. Buehrer, "RIS-aided localization under position and orientation offsets in the near and far field," submitted to *IEEE Trans. on Wireless Commun., available online: arxiv.org/abs/2210.03599*, 2022.

[2] ——, "Fundamentals of RIS-aided localization in the far-field," submitted to *IEEE Trans. on Wireless Commun., available online: arxiv.org/abs/2206.01652*, 2022.

[3] M. Z. Win, Z. Wang, Z. Liu, Y. Shen, and A. Conti, "Location awareness via intelligent surfaces: A path toward holographic NLN," *IEEE Veh. Technology Magazine*, vol. 17, no. 2, pp. 37–45, June 2022.

[4] S. Hu, F. Rusek, and O. Edfors, "Beyond massive MIMO: The potential of positioning with large intelligent surfaces," *IEEE Trans. on Signal Processing*, vol. 66, no. 7, pp. 1761–1774, Apr. 2018.

[5] Z. Wang, Z. Liu, Y. Shen, A. Conti, and M. Z. Win, "Location awareness in beyond 5G networks via reconfigurable intelligent surfaces," *IEEE J. Sel. Areas Commun.*, vol. 40, no. 7, pp. 2011–2025, July 2022.

[6] A. Elzanaty, A. Guerra, F. Guidi, and M.-S. Alouini, "Reconfigurable intelligent surfaces for localization: Position and orientation error bounds," *IEEE Trans. on Signal Processing*, vol. 69, pp. 5386–5402, Aug. 2021.

[7] D. Dardari, N. Decarli, A. Guerra, and F. Guidi, "LOS/NLOS near-field localization with a large reconfigurable intelligent surface," *IEEE Trans. on Wireless Commun.*, vol. 21, no. 6, pp. 4282–4294, June 2022.

[8] Z. Abu-Shaban, K. Keykhosravi, M. F. Keskin, G. C. Alexandropoulos, G. Seco-Granados, and H. Wymeersch, "Near-field localization with a reconfigurable intelligent surface acting as lens," in *Proc., IEEE Intl. Conf. on Commun. (ICC)*, 2021.

[9] A. Fascista, M. F. Keskin, A. Coluccia, H. Wymeersch, and G. Seco-Granados, "RIS-aided joint localization and synchronization with a single-antenna receiver: Beamforming design and low-complexity estimation," *IEEE J. of Sel. Topics in Signal Processing*, to appear.

[10] K. Keykhosravi, M. F. Keskin, S. Dwivedi, G. Seco-Granados, and H. Wymeersch, "Semi-passive 3D positioning of multiple RIS-enabled users," *IEEE Trans. on Veh. Technol.*, vol. 70, no. 10, pp. 11 073–11 077, Oct. 2021.

[11] K. Keykhosravi, M. F. Keskin, G. Seco-Granados, P. Popovski, and H. Wymeersch, "RIS-enabled SISO localization under user mobility and spatial-wideband effects," *IEEE J. of Sel. Topics in Signal Processing*, pp. 1–1, to appear.

[12] A.-A. A. Boulogeorgos, A. Alexiou, and M. Di Renzo, "Outage performance analysis of RIS-assisted UAV wireless systems under disorientation and misalignment," *arXiv:2201.12056*, 2022.

[13] S. M. LaValle, *Planning Algorithms*. Cambridge University Press, 2006.

[14] A. Shahmansoori, G. E. Garcia, G. Destino, G. Seco-Granados, and H. Wymeersch, "Position and orientation estimation through millimeter-wave MIMO in 5G systems," *IEEE Trans. on Wireless Commun.*, vol. 17, no. 3, pp. 1822–1835, Mar. 2018.

[15] R. A. Horn and C. R. Johnson, *Matrix Analysis*. Cambridge University Press, 2012.

[16] Y. Shen and M. Z. Win, "Fundamental limits of wideband localization — part I: A general framework," *IEEE Trans. on Info. Theory*, vol. 56, no. 10, pp. 4956–4980, Oct. 2010.

[17] F. Guidi and D. Dardari, "Radio positioning with EM processing of the spherical wavefront," *IEEE Trans. on Wireless Commun.*, vol. 20, no. 6, pp. 3571–3586, Jan. 2021.